Comparison of Different Techniques to Estimate Surface Soil Moisture

S. Farid F. Mojtahedi, Ali Khosravi, Behnaz Naeimian, S. Adel A. Hosseini

Abstract**—**Land subsidence is a gradual settling or sudden sinking of the land surface from changes that take place underground. There are different causes of land subsidence; most notably, ground-water overdraft and severe weather conditions. Subsidence of the land surface due to ground water overdraft is caused by an increase in the intergranular pressure in unconsolidated aquifers, which results in a loss of buoyancy of solid particles in the zone dewatered by the falling water table and accordingly compaction of the aquifer. On the other hand, exploitation of underground water may result in significant changes in degree of saturation of soil layers above the water table, increasing the effective stress in these layers, and considerable soil settlements. This study focuses on estimation of soil moisture at surface using different methods. Specifically, different methods for the estimation of moisture content at the soil surface, as an important term to solve Richard's equation and estimate soil moisture profile are presented, and their results are discussed through comparison with field measurements obtained from Yanco1 station in south-eastern Australia. Surface soil moisture is not easy to measure at the spatial scale of a catchment. Due to the heterogeneity of soil type, land use, and topography, surface soil moisture may change considerably in space and time.

Keywords**—**Artificial neural network, empirical method, remote sensing, surface soil moisture, unsaturated soil.

I. Introduction

LAND subsidence is a complicated geological problem which may cause serious damages to environment or human life [1]. The damages associated with subsidence include hurricane surge, freshwater flooding, and perhaps geologic growth fault activation, cracking of buildings, misalignment of bridge abutments, roads, railways, storm sewers or other underground pipelines, collapse of well casings, conduits, water-storage installations [2], [3]. A slow decline in the land elevation is named land subsidence, which is resulted from a number of reasons, most notably the excess withdrawal of groundwater and climate changes as natural causes of the phenomenon [1]. The excessive pumping of ground water may result in compression of underground materials in aquifers due to declining water tables [3], [4]. It may also change the soil's moisture content profile of upper layers and their saturation conditions. Soil's degree of saturation has direct influence on interparticle contact forces between the soil's grains and its state of stress.

Accordingly, considerable changes in soil's volume in different layers are expected as a result of degree of saturation change. Over the past three decades, quite extensive research has been performed on the measurement of land subsidence as a result of compaction of aquifer. However, the effects that degree of saturation change may have on soil's stress state, and deformation behavior in such an event has not been fully understood. Reasons for this lack of knowledge are difficulties associated with in-situ measurements of moisture content and deformation. Soil moisture content profile is usually estimated through the use of Richard's equation. Richard's equation is a nonlinear partial differential equation, with no closed-form analytical solution. Its accurate estimation of soil's moisture content requires proper measurement of initial soil's moisture content and soil's hydraulic and mechanical properties. Specifically, the moisture content at the surface is one of the important terms for this purpose. Different techniques have been developed over the past decade for the measurement or estimation of soil moisture content at the surface because of problems facing measuring soil moisture. For instance, in situ point observation can cover only limited area, which wide region cannot be represented by [5].

Over the past decade, technological advances in remote-sensing result in development of different techniques for measuring surface soil moisture in a wide area and at different time scales [6]. It is also more efficient for estimating surface soil moisture at a large scale. The empirical interpretation of the relationship between the normalized difference vegetative index (NDVI) and land surface temperature (LST) has widely been applied for soil moisture monitoring [7]-[9]. As another approach of using satellite remote sensing in order to avoid the direct method of gathering surface soil moisture, there are radar backscattering models that use radar images provided by synthetic aperture radars (SARs) to estimate surface soil moisture. SARs are highly sensitive to the dielectric constant of soils and the surface soil moisture content. Different theoretical [10] and empirical [11], [12] models presented in literature over the past decade to define correlation between radar backscatter coefficients and soil moisture. These techniques were observed to provide adequate estimation of soil moisture. However, their estimations highly rely on surface roughness and vegetation cover. For example, [13] investigated the effect of different bands of radar signals on results of different models and checked their accuracy and [14] used Dubois model in order to map surface soil moisture.

The use of Hydrological practice SVAT (Soil-Vegetation-Atmosphere-Transfer) models is another way of estimating surface soil moisture. Incorporating different formulations of drainage and evapotranspiration, these models are very helpful ways to circumvent issues regarding vegetation cover. [15],

A. Khosravi, F. Mojtahedi, B. Naeimian and A. Ahmadi Hosseini are with the Civil Engineering Department, Sharif University of Technology, Tehran, Iran (phone: +98-21-66164208; e-mail: khosravi@sharif.edu, farid.fazel.m@gmail.com, bhnz.naeimian@gmail.com, a.ahmadihosseini@gmail.com,).

[16] used this method in different places for finding soil moisture and checked its adequacy. They also incorporate empirical formulations to consider the effect of weather conditions and seasonal changes on surface soil moisture measurements. Hard formulation of empirical models makes surface soil moisture estimation a complex and nonlinear process. This complexity makes it suitable for the use of artificial neural network. The neural networks are tools used in the retrieval of geophysical parameters. Studies have been made in past in order to check the adequacy of using neural networks for estimating soil properties [17]-[22]. The adequacy of output parameters is dependent on the quality of the parameters used to train the neural network [23], [24].

This study provides the results of soil moisture content at the surface estimated using three different approaches, TVDI using MODIS data, empirical model, and artificial neural network, and their reliability in reproducing the temporal evolution of soil moisture observed in an experimental plot located in south-eastern Australia. The models accuracy was tested during year 2007 and compared with each other.

II. Description of Area

A. Study Area

The Yanco study area shown in Fig. 1 is a semi-arid agricultural area of approximately 60 km by 60 km, characterized by flat topography (Fig. 1); its land use is mainly grazing dry lands with occasional winter crops (barley, wheat, canola, and oats). There are 37 site stations in study area. Station Yanco1 is located at latitude -34.62888 and longitude 145.84895 with elevation of 120 m shown in Fig. 2 and Fig. 3 [25]. Annual precipitation is 416 mm, and the evapotranspiration is 1188 mm. The main components of soil texture are silt and loam with details presented in Table I.

TABLE I
Soil Properties for Yanco1

Soil type	Density (g/cm^3)	Sand (%)	Silt (%)	Clay (%)
Silt & loam	1.41	54.55	32.11	13.34

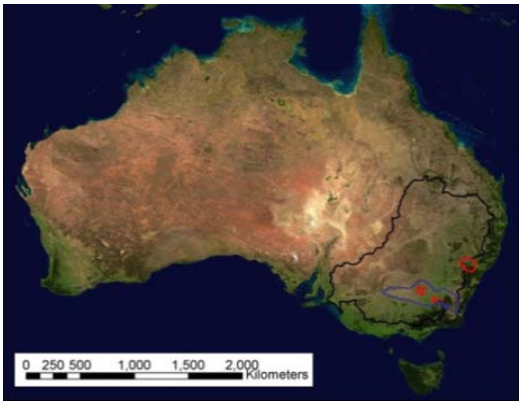

Fig. 1 Location map of the study area in south-eastern Australia [25]

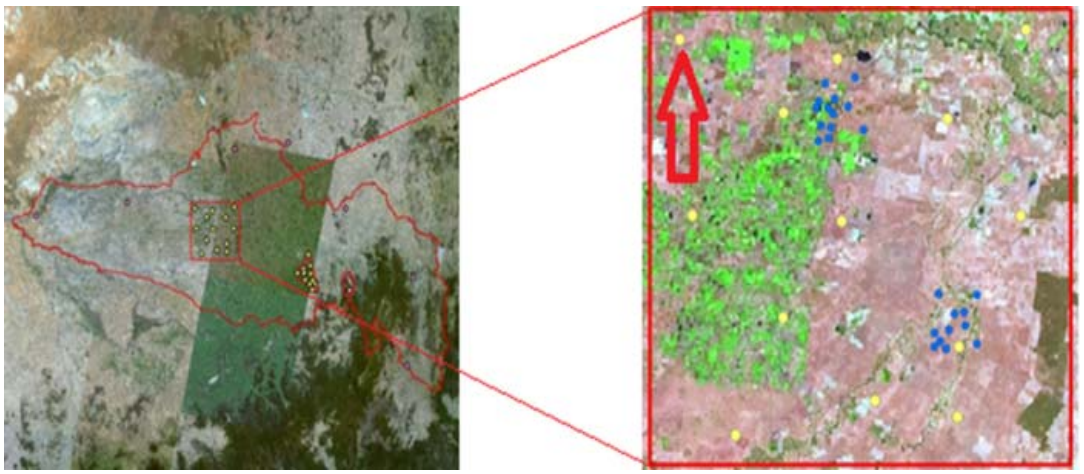

Fig. 2 Land cover of the study area. Dots are showing the stations. The yellow sites have a different instrumentation compared to the blue ones. The yellow site shown with a fingerpost is Yanco1 [25]

B. Instruments

Project variables that are monitored on the project site are as:

- Precipitation is monitored by a Hydrological Service TB4 rain gauge with a resolution of 0.2 mm.
- Soil moisture which is monitored by three Campbell Scientific CS-616 at depth 0-30 cm, 30-60 cm and 60-90 cm shown in Fig. 4 and one Stevens at depth 0-5.7 cm.
- Temperature of soil by a Hydra-Probe thermistor at depth 3 cm and a T-107 thermistor at 15 cm.
- Groundwater table with an Odyssey capacitance probe with 2 m length.
- The variables which are periodically monitored at these sites are used for calibration as:
- Gravity which is monitored by a Scintrex CG-3M Autograv relative gravimeter.
- Soil moisture by three connector TDR soil moisture probes at depth 0-30 cm, 30-60 cm and 60-90 cm and a CPN 503DR Hydro probe neutron moisture meter that

measures from the surface to groundwater or bottom of piezometer.

- Groundwater table by using an electronic water level measuring tape.

Schematic of instruments used at site is shown in Fig. 5.

Fig. 3 Yanco1 station and instruments [25]

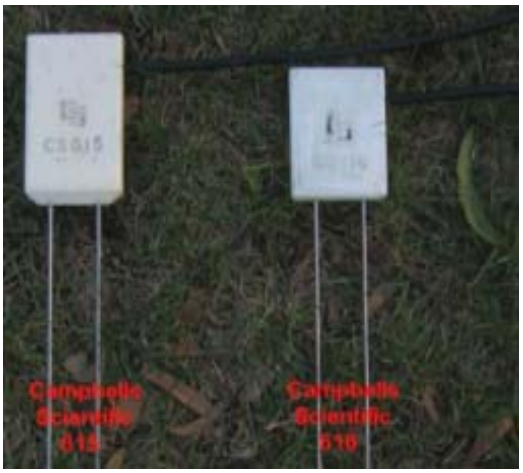

Fig. 4 CS-616 soil moisture probe [25]

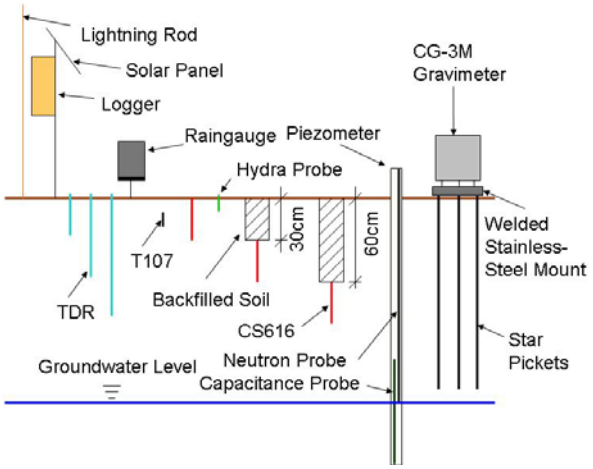

Fig. 5 Schematic of instruments at site [25]

III. Methodologies to Estimate Moisture Content at the Soil Surface

A. Remote Sensing

1. Use of Thermal Images (MODIS data)

a. n^{th} Order Polynomial Relations

Triangle method derives land surface soil moisture from NDVI and LST. NDVI characterizes the greenness of vegetation indicating water stress and is calculated using:

$$NDVI = \frac{(NIR - VIS)}{(NIR + VIS)} \tag{1}$$

where VIS stands for the spectral reflectance measurements in the visible (red) and NIR for near-infrared regions. This spectral reflectance is ratio of reflected over the incoming radiation in spectral band individually, ranging between 0.0 to 1.0. NDVI was derived directly from MODIS product (MOD13A2) and LST was derived from MODIS products. The MODIS LST product (MOD11A1) provides per-pixel temperature on a daily basis. Averaged temperatures are extracted in Kelvin. These values, NDVI and LST, are extracted using ENVI.

When the scattered data of scaled NDVI and LST are plotted, the shape of the graph resembles a triangle as presented in Fig. 6. The abscissa and the ordinate of the curve are scaled as NDVI and LST, respectively:

$$N^* = \frac{(NDVI - NDVI_{\min})}{(NDVI_{\max} - NDVI_{\min})} \tag{2}$$

$$T^* = \frac{(T_s - T_{\min})}{(T_{\max} - T_{\min})} \tag{3}$$

NDVI and T_s are the observed NDVI and the observed land surface temperature, respectively. The retrieved MODIS images using ENVI, and min. and max. values for each parameter represent the minimum and maximum values of the pixels inside the triangle. $NDVI_{min}$ and T_{max} resemble for bare soil, while $NDVI_{max}$ and T_{min} are related to full vegetation.

High soil moisture content is represented at the right side of the curve, while at the left side the surface soil moisture is low. The slope shows that as the NDVI increases, the LST decreases. This negative relation between these two parameters shows that bare soil (with low NDVI) is warmer than soil with high vegetation cover. The maximum vegetation is at the apex of the triangle, but the corresponding value of LST is low with very little variation. This variation in LST with high NDVI (at the apex of the triangle) is due to wetness of soil moisture in the vegetation [26]. Therefore, the soil surface dryness or wetness is reflected by the variation in temperature [27].

A regression formula has been represented by [28] using scaled NDVI and LST to estimate surface soil moisture:

$$M = \sum_{i=0}^{i=n} \sum_{j=0}^{j=n} a_{ij} NDVI^{*(i)} T^{*(j)} \quad (4)$$

In this paper, the second or third order polynomials are studied which represent more accuracy than a single polynomial; while a single polynomial is able to represent a wide range of surface climate conditions and land surface types.

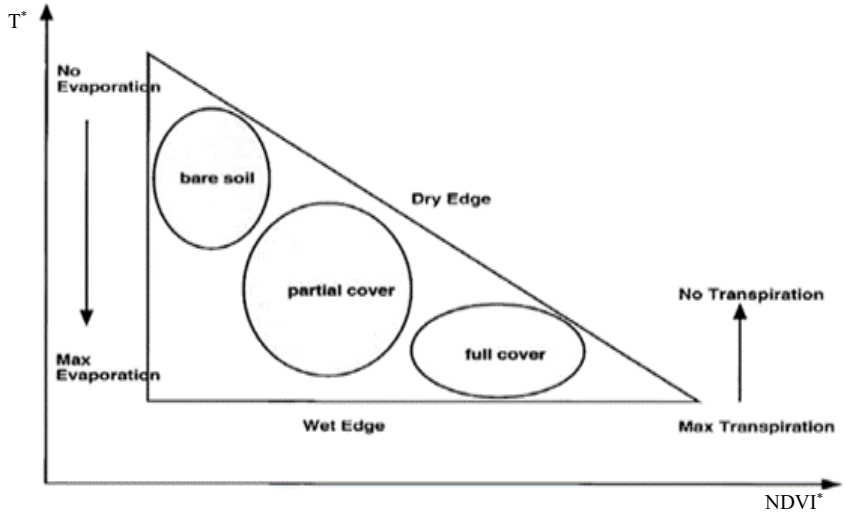

Fig. 6 Triangular relationship between soil moisture, LST and NDVI [8]

NDVI was replaced by fractional vegetation (Fr) [29], [30]. Fr is an important parameter that has key role in the energy exchanges at the land surface; it measures how much the land surface is covered by vegetation. Equation (5) shows the developed method by Gillies et al. using NDVI to determine Fr [29]:

$$Fr = \left(\frac{NDVI - NDVI_{\min}}{NDVI_{\max} - NDVI_{\max}} \right)^2 \quad (5)$$

3rd order polynomial relation algorithm with Fr:

$$M = \sum_{i=0}^{i=3} \sum_{j=0}^{j=3} a_{ij} Fr^{*(i)} T^{*(j)} \quad (6)$$

b. TVX Method

Another approach uses the slope between NDVI and LST of 3×3 pixels (station is central pixel) in a particular day and represents a method using the TVX slope, assuming a linear relation between NDVI and LST. In addition to MODIS data, another dataset is needed to run the algorithm, so a linear relation between MODIS data (NDVI and LST) and a specific meteorology data is assumed. With these assumptions, surface soil moisture at the surface can be obtained by using (7)-(11):

$$M = a_0 + a_1 Sl + a_2 Ev_5 \quad (7)$$

$$M = a_0 + a_1 Sl + a_2 Ev_{10} \quad (8)$$

$$M = a_0 + a_1 Sl + a_2 Rain \quad (9)$$

$$M = a_0 + a_1 Sl + a_2 Tem \quad (10)$$

$$M = a_0 + a_1 Sl + a_2 Ev_5 + a_3 Rain \quad (11)$$

Sl : the slope of linear relation between NDVI and LST; Ev5: cumulative evaporation for past 5 days; Ev10: cumulative evaporation for past 10 days; Tem: air temperature; Rain: the amount of rainfall in a particular day.

2. Using SAR Images

a. Integral Equation Model (IEM)

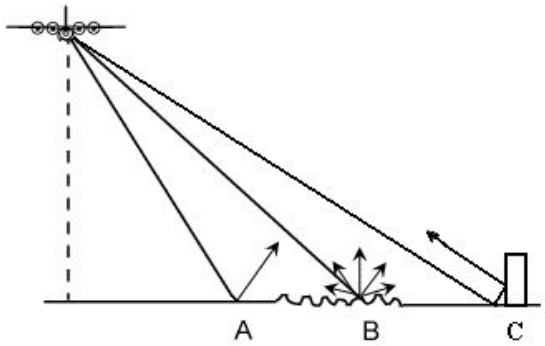

Fig. 7 Backscattering from different surfaces

IEM is a theoretical model based on backscattering coefficients. The backscattering coefficients ($\sigma°_{HH}$, $\sigma°_{VV}$) are parameters describing the ratio of scatters received to scatters that were sent to a specific point and are highly dependent on the vegetation cover in the area (Fig. 7). The expressions for these coefficients consist of the angle of incidence (θ), the dielectric constant (ε), the standard deviation of surface height

(h_{rms}), the relative permeability (μ_r), and the wave number (k) and are defined as:

$$\sigma_{pp}^{o} = \frac{k^2}{4\pi} e^{-2k^2 h_{rms}^2 \cos^2\theta} \sum_{n=1} |I_{pp}^{n}| \frac{W^{(n)}(2k.\sin\theta.0)}{n!} \quad (12)$$

$$I_{pp}^{n} = (2k.h_{rms}.\cos\theta) f_{pp} e^{-2k^2 h_{rms}^2 \cos^2\theta} + (k.h_{rms}.\cos\theta)^n F_{pp} \quad (13)$$

where $\sigma°_{PP}$ is the backscattering coefficient of pp polarization (HH or VV), and f_{PP} and F_{PP} are defined as:

$$f_{HH} = \frac{-2R_H}{\cos\theta} \quad (14)$$

$$f_{VV} = \frac{2R_V}{\cos\theta} \quad (15)$$

$$F_{HH} = -\left[\left(\frac{\sin^2\theta}{\cos\theta} - \frac{\sqrt{\mu_r\varepsilon - \sin^2\theta}}{\mu_r}\right)(1+R_H)^2 - 2\sin^2\theta\left(\frac{1}{\cos\theta} - \frac{1}{\sqrt{\mu_r\varepsilon - \sin^2\theta}}\right)(1+R_H)(1-R_H) + \left(\frac{\sin^2\theta}{\cos\theta} - \frac{\mu_r(1+\sin^2\theta)}{\sqrt{\mu_r\varepsilon - \sin^2\theta}}\right)(1-R_H)^2\right] \quad (16)$$

$$F_{VV} = \left[\left(\frac{\sin^2\theta}{\cos\theta} - \frac{\sqrt{\mu_r\varepsilon - \sin^2\theta}}{\varepsilon}\right)(1+R_V)^2 - 2\sin^2\theta\left(\frac{1}{\cos\theta} - \frac{1}{\sqrt{\mu_r\varepsilon - \sin^2\theta}}\right)(1+R_V)(1-R_V) + \left(\frac{\sin^2\theta}{\cos\theta} - \frac{\varepsilon(1+\sin^2\theta)}{\sqrt{\mu_r\varepsilon - \sin^2\theta}}\right)(1-R_V)^2\right] \quad (17)$$

In (14)-(17), R_H and R_V are the horizontally and vertically polarized Fresnel reflection coefficients, respectively which are defined as:

$$R_H = \frac{\cos\theta - \sqrt{\varepsilon - \sin^2\theta}}{\cos\theta + \sqrt{\varepsilon - \sin^2\theta}} \quad (18)$$

$$R_V = \frac{\varepsilon\cos\theta - \sqrt{\varepsilon - \sin^2\theta}}{\varepsilon\cos\theta + \sqrt{\varepsilon - \sin^2\theta}} \quad (19)$$

and $W^{(n)}$ is the Fourier transform of the n^{th} power of the surface correlation function.

Using (12)-(19) and with the help of high correlation between dielectric constant and soil's moisture, the surface soil moisture can be calculated.

b. Dubois Model

Using scatter meter data for modeling radar backscattering coefficient, [11] suggested a semi-empirical model for $\sigma°_{HH}$ and $\sigma°_{VV}$ as:

$$\sigma°_{HH} = 10^{-2.75}\left(\frac{\cos^{1.5}\theta}{\sin^5\theta}\right)10^{0.028.\varepsilon.\tan\theta} (k.h_{rms}.\sin\theta)^{1.4}\lambda^{0.7} \quad (20)$$

$$\sigma°_{VV} = 10^{-2.35}\left(\frac{\cos^3\theta}{\sin^3\theta}\right)10^{0.046.\varepsilon.\tan\theta} (k.h_{rms}.\sin\theta)^{1.1}\lambda^{0.7} \quad (21)$$

where h_{rms} and ε are the standard deviation of surface height and the dielectric constant, respectively (as unknowns of the equations), θ is the angle of incidence, and λ is the wavelength. θ and λ are two known parameters that can be gathered directly, using SAR images.

From (20) and (21), there are two unknowns (ε, h_{rms}) that can be calculated with solving these, and by gathering ε, we can calculate the surface soil moisture with high correlation which exists between soil moisture and dielectric constant.

c. Oh Model

Based on backscattering methods for evaluation of soil moisture, a semi-empirical model was presented and developed [12], [31]-[33]. Co-polarized and cross-polarized backscattering ratios are used in order to raise the functionality of the model. The expressions for co-polarized and cross polarized backscattering ratios are as:

$$p = \frac{\sigma°_{HH}}{\sigma°_{VV}} = 1 - \left(\frac{\theta}{90°}\right)^{0.35M^{-0.65}} e^{-0.4(k.h_{rms})^{1.4}} \quad (22)$$

$$q = \frac{\sigma°_{HV}}{\sigma°_{VV}} = 0.095(0.13 + \sin 1.5\theta)^{1.4}\left(1 - e^{-1.3(k.h_{rms})^{0.9}}\right) \quad (23)$$

$$\sigma°_{VH} = 0.11M^{0.7}(\cos\theta)^{2.2}\left(1 - e^{-0.32(k.h_{rms})^{1.8}}\right) \quad (24)$$

where θ is the angle of incidence, h_{rms} is the standard deviation of surface height, k is the wave number, and M is the volumetric moisture content. By solving (22)-(24), the surface soil moisture (M) can be simply calculated.

B. Empirical Method

Reference [16] suggested the use of water balance equations for modeling moisture temporal pattern. It is assumed the upper soil layer of thickness L as a lumped system, in which water balance equations can be presented as:

$$\frac{dW(t)}{dt} = f(t) - e(t) - g(t) \tag{25}$$

where: W: amount of water existing in the soil layer; W_{max}: maximum water capacity of the soil layer; f: portion of precipitation infiltrating into the soil layer; e: evapotranspiration rate; g: drainage rate due to interflow or deep percolation.

The expression for W involves the volumetric water content (θ) and residual volumetric water content (θ_r):

$$W(t) = \left[\theta(t) - \theta_r\right]L \tag{26}$$

The infiltration (f) is estimated using Green–Ampt equation:

$$f(t) = K_s\left[1 - \frac{\psi\left(\theta_s - \theta'_i\right)}{F}\right] \tag{27}$$

where: K_s: saturated hydraulic conductivity; Ψ: wetting front soil suction head; θ'_i: soil water content at the beginning of the rainfall (rainfall is assumed to be uniform); F: cumulated infiltration depth from the beginning of the rainfall.

A non-linear relation of W is used in order to estimate the drainage parameter (g):

$$g(t) = K_s\left[\frac{W(t)}{W_{\max}}\right]^{3+\left(\frac{2}{\lambda}\right)} \tag{28}$$

where λ is the pore size distribution index related to the soil layer structure. In order to use (28), the flow is assumed to be gravity driven, with drainage consisting of deep percolation.

Evapotranspiration rate (e) in the soil layer is given by linear relation with potential evapotranspiration (ET_p):

$$e(t) = ET_p(t)\frac{W(t)}{W_{\max}} \tag{29}$$

ET_p is estimated by using the developed empirical relation [34]:

$$ET_p(t) = a + b\left[\xi\left(0.46T_a(t) + 8.13\right)\right] \tag{30}$$

where: Ta: mean air temperature; ξ: percentage of total daytime hours for the period used out of total daytime hours of the year; a, b: parameters that need local calibration.

C. Artificial Neural Network

A neural network is a mathematical model consisting of interconnected neurons (nodes) that assimilate the functioning of biological neurons. They are used as nonlinear statistical tools in modeling complex relationships between inputs and outputs (Fig. 8). In these techniques, the neurons are arranged in different layers with random weighted connections between layers. It is an adaptive system that changes its structure based on the external or internal information that flows through the network during the training phase. The development of the model involves two phases: training and testing. Training phase essentially selects one model from all the available ones that optimizes the cost function evaluated on the obtained training dataset. Test phase involves the assessment of the performance of the model using different evaluation procedures or a test dataset. Root mean square error is the cost function in this study.

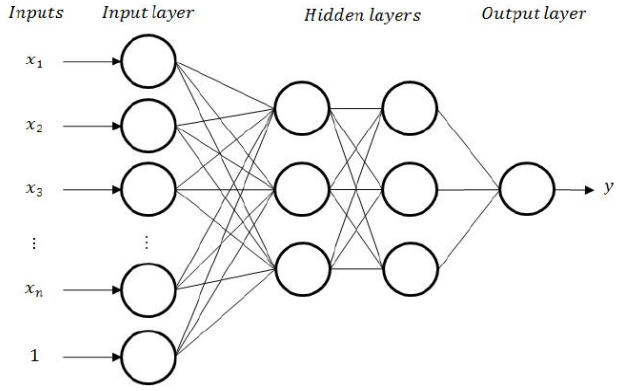

Fig. 8 A typical neural network

IV. Results and Discussion

The objective of this paper is to find the best way of estimating the surface soil moisture. Studies have been made over year 2007 in order to find the soil moisture with the use of different methods. Results of these methods are then compared to find the best solution for finding and estimating the surface soil moisture.

A. Remote Sensing

1. Using Thermal Images (MODIS Data)

a. n^{th} Order Polynomial Relations

By using triangle method, soil moisture is estimated from remote sensing by using derived NDVI and LST. Observing the ground's soil moisture and the MODIS data for the pixel matching the site of station in different time intervals gives (4), (6)-(11). An approach is presented for year 2007 as observed soil moisture, LST and NDVI of year 2007 were used. A strong correlation between the simulated and observed soil moisture is obtained from 2nd and 3rd order polynomial relations of the observed soil moisture with NDVI and LST, and also 3rd order polynomial relation of soil moisture with Fr.

The coefficients a_{ij} obtained after calibrations are calculated (Tables II-IV).

Based on the calibration, the 3rd order polynomial relation is found to be more accurate (Table V). It is recommended to calculate daily NDVI instead of 16 days mean product

(MOD13A2), which gives more accurate and better estimation of soil moisture. Measured and estimated surface soil moisture using n^{th} order polynomial relations are shown in Fig. 9.

TABLE II
COEFFICIENTS FOR 2ND ORDER POLYNOMIAL FOR YEAR 2007

a_{ij}	j=0	j=1	j=2
i=0	0	4.21	-4.07
i=1	8.40	-34.37	33.14
i=2	-14.02	56.81	-54.21

TABLE III
COEFFICIENTS FOR 3RD ORDER POLYNOMIAL WITH NDVI FOR YEAR 2007

a_{ij}	j=0	j=1	j=2	j=3
i=0	0	3.27	-3.44	-0.15
i=1	8.63	-37.94	48.83	-9.78
i=2	-12.85	52.44	-63.52	0.64
i=3	0.13	0.32	9.37	1.22

TABLE IV
COEFFICIENTS FOR 3RD ORDER POLYNOMIAL WITH FR FOR YEAR 2007

a_{ij}	j=0	j=1	j=2	j=3
i=0	0	0	0	-0.77
i=1	0	0	29.08	-16.54
i=2	0	-10.75	-8.99	16.98
i=3	30.74	-17.33	-71.02	65.36

TABLE V
RMSE FOR N^{TH} ORDER POLYNOMIAL RELATIONS

	RMSE for 2007
2^{nd} order polynomial relation	0.047
3^{rd} order polynomial relation with NDVI	0.046
3^{rd} order polynomial relation with Fr	0.046

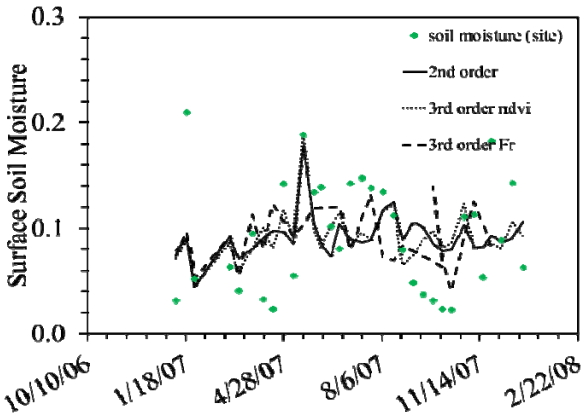

Fig. 9 Measured and estimated surface soil moisture using n^{th} order polynomial relations for 2007

b. TVX Model

This approach which combines MODIS data and daily meteorology data to estimate surface soil moisture is represented below. Daily meteorology data were provided by two sites Weather ground [35] and Bureau of Meteorology Australian Government [36] (i.e., rain, air temperature and evaporation). After extracting NDVI and LST of 3×3 pixels from the MODIS image of a particular day, the TVX slope is studied, and by adding meteorology data, five relations are obtained to estimate surface soil moisture (Table VI). the results are shown in Fig. 10.

TABLE VI
RMSE FOR TVX MODELS

Models number	Relations	RMSE
TVX mode1	$M=6.46 - 8.82\,Sl + 0.7Ev_5$	0.0471
TVX model 2	$M=6.57 - 8.95\,Sl + 0.04Ev_{10}$	0.0473
TVX model 3	$M=8.16 - 5.56\,Sl + 0.29Rain$	0.0476
TVX model 4	$M=3.32 - 10.76\,Sl + 0.32Tem$	0.0452
TVX mode 5	$M=5.42 - 6.46\,Sl + 0.1Ev_5 + 0.42Rain$	0.0451

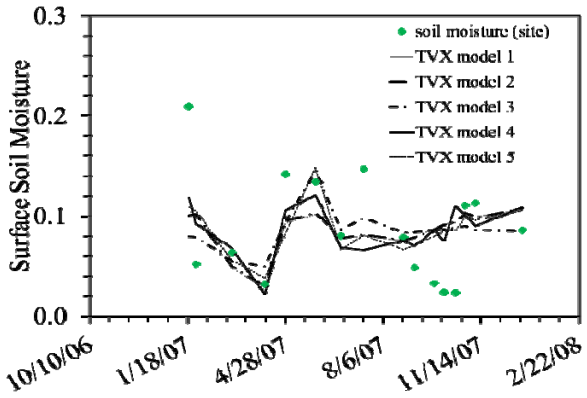

Fig. 10 Measured and estimated surface soil moisture using TVX method for year 2007

B. Empirical Model

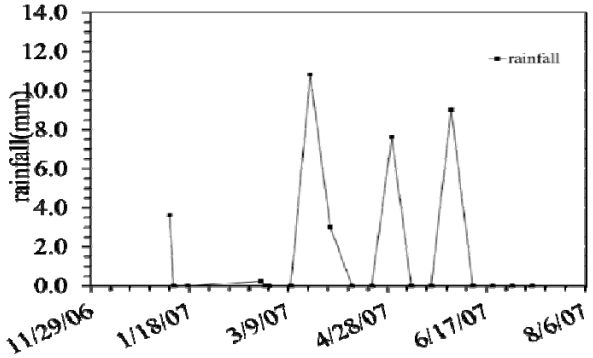

Fig. 11 Rainfall for 2007

Same as the other models, studies have been made in order to estimate surface soil moisture in 2007. The objective of this model is using water balance equations for finding soil moisture. As the effect of raining is seen in Figs. 11 and 12, most of the errors are in the times of raining. The RMSE value in a one-year interval, 2007 is 0.13.

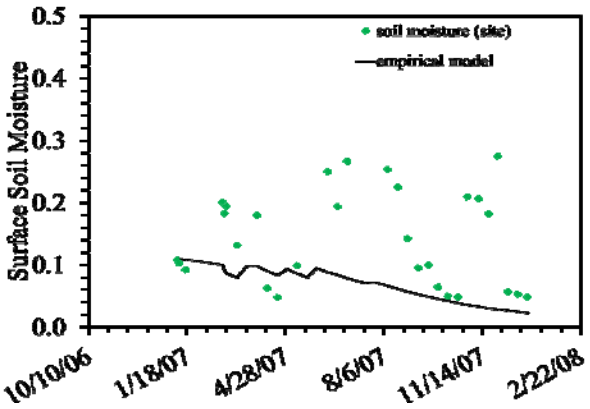

Fig. 12 Measured and estimated surface soil moisture using empirical model for year 2007

C. Neural Network

As shown in Fig. 13, artificial neural networks have been used to estimate soil moisture. Parameters that were used as input in neural networks consist of empirical methods equation and remote sensing parameters:

- Ev5: cumulative evaporation for past five days
- Tem: air temperature
- R: rain
- LST: land surface temperature
- NDVI: Normalized Difference Vegetation Index

These parameters were qualified in different combinations in order to gather the best results. The data are randomly divided into 70% for training, 15% for validation, and 15% for testing the trained network.

The best result in 2007 with use of artificial neural network was gathered when the input parameters were Tem, R, and NDVI. Because NDVI had low accuracy, normalized NDVI (N*) was used instead in surveying the year. The best result for this interval was gathered as 0.055 with the use of different functions.

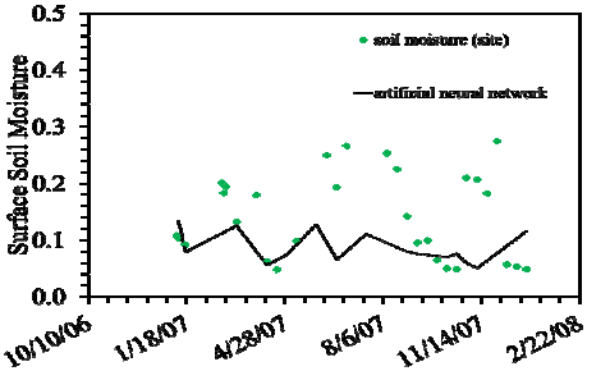

Fig. 13 Measured and estimated surface soil moisture using artificial neural network for 2007

To compare the presented models with each other, the best model from each method with the least RMSE is shown in Fig. 14. As it can be seen, models estimations in last three months of the year are closer to each other than the first three months of the year. In January, the regression model and TVX model are giving a better estimation of the surface soil moisture compared to the other models, but in March, artificial neural network and empirical model show better results. It could be understood that the existence of rain introduces error in the empirical model but gives the artificial neural network more accuracy. The existence of rain also makes using thermal images troublesome due to their mechanism of gathering images.

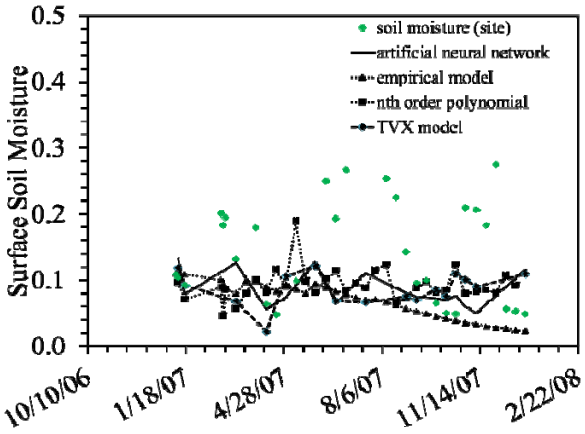

Fig. 14 Comparison of different methods

V. Conclusion

As land subsidence becomes a great concern, different methods are represented to investigate this issue. In order to simplify this process, a method is used for the soil moisture profile in different depths. As a way to find this profile, we can use surface soil moisture as a boundary condition. In this study, different methods were studied to estimate the surface soil moisture. Thermal images (MODIS data) were the main parameters of two methods: n^{th} order polynomial relations and TVX models; radar images were used in three methods: IEM, Oh model, and Dubois model. However, due to unavailability of images, models are not tested. Another approach was empirical method or artificial neural network. These models were verified over 2007. RMSE obtained from these methods was represented in the results in order to make a comparison. MODIS data are easy to provide but are very sensitive to clouds. Radar images circumvent weather conditions but getting access to radar data is difficult, which makes using radar backscattering models haywire in comparison with other models and high accessibility of their data.

The study demonstrated that the empirical method had a close relationship with the amount of rain, hence it might fail due to heavy rain precipitation. And due to high RMSE for year 2007, this method is not recommended to be used for long intervals like over a year. The problem of clouds and rain is solved by using artificial neural network. Existence of high vegetation cover leads to intense errors in calculated surface soil moistures. Although requirements of artificial neural network and empirical method are more available, which leads to more utilization, remote sensing gives a better estimation with less error.

REFERENCES

[1] Y. Cui, et al. "Development and application of a regional land subsidence model for the plain of Tianjin." Journal of Earth Science 25.3 (2014): 550-562.

[2] Y. Najjar, Z. Musharraf, "Surface subsidence prediction by nonlinear finite-element analysis." Journal of geotechnical engineering 119.11 (1993): 1790-1804.

[3] H. Bouwer, "Land Subsidence and Cracking Due to Ground-Water Depletion." Ground Water 15.5 (1977): 358-364.

[4] Thu, Trinh M., and Delwyn G. Fredlund. "Modelling subsidence in the Hanoi city area, Vietnam." Canadian Geotechnical Journal 37.3 (2000): 621-637.

[5] Ahmad, M. F., S. Runping, and Y. Jing. "Soil Moisture Retrieval through Satellite Data for Gansu and Xinjiang Region of China." Pakistan Journal of Meteorology (Pakistan) (2012).

[6] Engman, Edwin T. "Progress in microwave remote sensing of soil moisture." Canadian Journal of Remote Sensing 16.3 (1990): 6-14.

[7] Patel, N. R., et al. "Assessing potential of MODIS derived temperature/vegetation condition index (TVDI) to infer soil moisture status." International Journal of Remote Sensing 30.1 (2009): 23-39.

[8] Sandholt, Inge, Kjeld Rasmussen, and Jens Andersen. "A simple interpretation of the surface temperature/vegetation index space for assessment of surface moisture status." Remote Sensing of environment 79.2 (2002): 213-224.

[9] Sun, W., et al. "Using the vegetation temperature condition index for time series drought occurrence monitoring in the Guanzhong Plain, PR China."International Journal of Remote Sensing 29.17-18 (2008): 5133-5144.

[10] Fung, A.K., Li, Z., and Chen, K.S. 1992. Backscattering from a randomly rough dielectric surface. IEEE Transactions on Geoscience and Remote Sensing, Vol. 30, No. 2, 356369. doi: 10.1109/36.134085.

[11] Dubois, P.C., van Zyl, J., and Engman, T. 1995. Measuring soil moisture with imaging radar. IEEE Transactions on Geoscience and Remote Sensing, Vol. 33, No. 6, pp. 915926. doi: 10.1109/TGRS.1995.477194.

[12] Oh, Y., Sarabandi, K. and Ulaby, F.T., 1992, An empirical model and an inversion technique for radar scattering from bare soil surfaces. IEEE Transactions on Geoscience and Remote Sensing, 30, pp. 370–382.

[13] Khabazan, S., M. Motagh, and M. Hosseini. "Evaluation of Radar Backscattering Models IEM, OH, and Dubois using L and C-Bands SAR Data over different vegetation canopy covers and soil depths." ISPRS—International Archives of the Photogrammetry, Remote Sensing and Spatial Information Sciences (2013): 225-230.

[14] Leconte, Robert, et al. "Mapping near-surface soil moisture with RADARSAT-1 synthetic aperture radar data." Water Resources Research 40.1 (2004).

[15] Famiglietti JS, Wood EF. 1994. Multiscale modeling of spatially variable water and energy balance processes. Water Resources Research 11: 3061–3078.

[16] Brocca, L., F. Melone, and T. Moramarco. "On the estimation of antecedent wetness conditions in rainfall–runoff modelling." Hydrological Processes22.5 (2008): 629-642.

[17] Baghdadi, N., Gaultier, S., and King, C.: Retrieving surface roughness and soil moisture from SAR data using neural networks, Can. J. Remote Sens., 28, 701–711, 2002a.

[18] Notarnicola, C., Angiulli, M., and Posa, F.: Soil moisture retrieval from remotely sensed data: neural network approach versus Bayesian method, IEEE T. Geosci. Remote Se., 46, 547–557, 2008.

[19] Paloscia, S., Macelloni, G., Santi, E., and Tedesco, M.: The capability of microwave radiometers in retrieving soil moisture profiles: an application of Artificial Neural Networks, Proceeding IEEEIGARSS, Firenze, Italy, 3, 1390–1392, 2002.

[20] Paloscia, S., Pampaloni, P., Pettinato, S., and Santi, E.: A comparison of algorithms for retrieving soil moisture from ENVISAT/ASAR images, IEEE T. Geosci. Remote Se., 46, 3274– 3284, doi:10.1109/TGRS.2008.920370, 2008.

[21] Paloscia, S., Pampaloni, P., Pettinato, S., and Santi, E.: Generation of soil moisture maps from ENVISAT/ASAR images in mountainous areas: a case study, Int. J. Remote Se., 31, 2265–2276, 2010.

[22] Santi, E., Paloscia, S., Pampaloni, P., Pettinato, S., and Poggi, P.: Retrieval of Soil Moisture from Envisat ASAR Images: A Comparison of Inversion Algorithms. Proceedings of the 2004 Envisat & ERS Symposium (ESA SP-572), 6–10 September 2004, Salzburg, Austria, 2004.

[23] Chai, Soo-See, et al. "Backpropagation neural network for soil moisture retrieval using NAFE'05 data: a comparison of different training algorithms." Int Archives Photogramm, Remote Sens Spatial Inf Sci (China) 37 (2008): 1345.

[24] Lakhankar, Tarendra, et al. "Non-parametric methods for soil moisture retrieval from satellite remote sensing data." Remote Sensing 1.1 (2009): 3-21.

[25] Smith, A. B., Walker, J. P., Western, A. W., Young, R. I., Ellett, K. M., Pipunic, R. C., Grayson, R. B., Siriwidena, L., Chiew, F. H. S. and Richter, H. The Murrumbidgee Soil Moisture Monitoring Network Data Set. Water Resources Research, vol. 48, W07701, 6pp., 2012 doi:10.1029/2012WR011976.

[26] Mekonnen, D. F. "Satellite remote sensing for soil moisture estimation: Gumara catchment, Ethiopia." International Institute for Geo-Information Science and Earth Observation, Enschede (2009).

[27] Carlson, Toby. "An overview of the" triangle method" for estimating surface evapotranspiration and soil moisture from satellite imagery." Sensors7.8 (2007): 1612-1629.

[28] Carlson, Toby N., Robert R. Gillies, and Eileen M. Perry. "A method to make use of thermal infrared temperature and NDVI measurements to infer surface soil water content and fractional vegetation cover." Remote sensing reviews 9.1-2 (1994): 161-173.

[29] Gillies, R. R., W. P. Kustas, and K. S. Humes. "A verification of the'triangle'method for obtaining surface soil water content and energy fluxes from remote measurements of the Normalized Difference Vegetation Index (NDVI) and surface e." International journal of remote sensing 18.15 (1997): 3145-3166.

[30] Quattrochi, Dale A., and Jeffrey C. Luvall. Thermal remote sensing in land surface processing. CRC Press, 2004.

[31] Oh, Y., Sarabandi, K. and Ulaby, F.T., 1994, An inversion algorithm for retrieving soi moisture and surface roughness from polarimetric radar observation. Proceedings IGARSS'94, Pasadena, USA. IEEE catalog no. 94CH3378-7, III, pp. 1582– 1584, (New York: IEEE).

[32] Oh, Y., Sarabandi, K. and Ulaby, F.T., 2002, Semi-empirical model of the ensemble-averaged differential Mueller matrix for microwave backscattering from bare soil surfaces. IEEE Transactions on Geoscience and Remote Sensing, 40, pp. 1348–1355.

[33] Oh, Y., 2004, Quantitative retrieval of soil moisture content and surface roughness from multipolarized radar observations of bare soil surfaces. IEEE Transactions on Geoscience and Remote Sensing, 42, pp. 596–601.

[34] Doorenbos J, Pruitt WO. 1977. Background and development of methods to predict reference crop evapotranspiration (ETo). In Crop Water Requirements. FAO Irrigation and Drainage Paper No. 24, FAO: Rome; 108–119 (Appendix II).

[35] Weather Forecast & Reports – Long Range & Local | Wunderground | Weather Underground, http://www.wunderground.com/ Accessed on 2/05/2016.

[36] Australia's official weather forecasts & weather radar, http://www.bom.gov.au/ Accessed on 9/05/2016.